

# Multivalent RGD synthetic peptides as potent $\alpha_v\beta_3$ integrin ligands†

Elisabeth Garanger,<sup>a,b</sup> Didier Boturyn,<sup>a</sup> Jean-Luc Coll,<sup>b</sup> Marie-Christine Favrot<sup>b</sup> and Pascal Dumy<sup>\*a</sup>

Received 13th December 2005, Accepted 14th February 2006

First published as an Advance Article on the web 3rd April 2006

DOI: 10.1039/b517706e

We study herein the multivalency effect of a cluster of  $\alpha_v\beta_3$ -ligands held on a cyclodecapeptide template. An array of RAFT(*c*[-RGDfK-])<sub>n</sub> derivatives containing from one to sixteen clustered RGD motifs were synthesized and comparatively assayed *in vitro* on  $\alpha_v\beta_3$ -expressing cells. Efficient inhibition of the  $\alpha_v\beta_3$ -specific 23C6 monoclonal antibody fixation was observed with ligands displaying three and four copies of the *cyclo*[-RGDfK-] peptide.

## Introduction

Integrins constitute an important family of transmembrane receptors involved in cell–cell/cell–matrix interactions and are central players in outside-in and inside-out signal transduction pathways.<sup>1</sup> The  $\alpha_v\beta_3$  heterodimer, known as the vitronectin receptor, is selectively overexpressed on the surface of endothelial cells of growing blood vessels and hence has been identified as a target in pathologies in which angiogenesis is stimulated.<sup>2</sup> In malignant tumours,  $\alpha_v\beta_3$  receptors are overexpressed in neocapillaries and, in certain cases, also on tumour cells (e.g. 25% of lung cancers). This led many groups to design selective Arginine-Glycine-Aspartate (RGD)-containing ligands to specifically target the tumour-associated  $\alpha_v\beta_3$  receptors. Among the monovalent ligands designed, the leader compound is the cyclic pentapeptide *cyclo*[-RGDf(NMe)V-] (Cilengitide) developed by Merck KGa.<sup>3</sup> This compound has recently entered phase II clinical trials as anti-angiogenic agent. The rationale for the development of multivalent ligands derives from the wide diversity of natural processes that involve multivalent ligand/receptor interactions.<sup>4</sup> Multivalency enhances the binding strength of a ligand to its receptor and promotes receptor-mediated internalisation of the bound entity. Recently, oligomeric compounds containing RGD moieties based on a polylysine core were reported<sup>5</sup> and biologically evaluated.<sup>6</sup> RGD-polymers seem promising ligands for imaging or therapeutic approaches.<sup>7</sup> At the same time, our group developed a tetrameric RGD structure named RAFT(*c*[-RGDfK-])<sub>4</sub> (Fig. 1).<sup>8</sup>

This compound contains a cluster of four copies of the *cyclo*[-RGDfK-] monomer<sup>9</sup> supported on a cyclic decapeptide scaffold (RAFT, Regioselectively Addressable Functionalised Template).<sup>10</sup> The major advantage of the RAFT comes from its two distinct addressable domains (upper and lower face of the template). These enable the simultaneous coupling of biomolecules (e.g. labelling or cytotoxic agents) to the RAFT(*c*[-RGDfK-])<sub>4</sub> structure for future

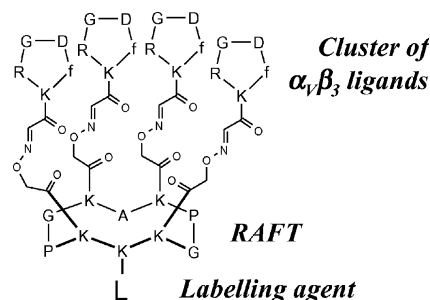


Fig. 1 Chemical structure of the tetraivalent RGD ligand RAFT(*c*[-RGDfK-])<sub>4</sub> conjugated to a label.

applications in vectorisation strategies. The spatial separation of both domains additionally prevents the molecules from the lower face from interfering with the targeting functions. This compound turned out to be highly efficient in targeting specifically tumour neo-vasculature as well as  $\alpha_v\beta_3$ -expressing metastases on murine animal models.<sup>11</sup> Cellular uptake was shown *in vitro* to occur through a receptor-mediated endocytosis contrasting with the fate of the cognate monovalent *cyclo*[-RGDfK-] peptide, which is internalised through an independent-fluid phase endocytosis.<sup>12</sup>

The present work aimed at studying the effect of the multivalency parameter in terms of interaction between the ligand and the target receptor and examining the contribution of each *c*[-RGDfK-] motif. For this purpose, we designed an array of RAFT(*c*[-RGDfK-])<sub>n</sub> derivatives containing from one to four copies of the *c*[-RGDfK-] monomer (compounds 1–4) (Fig. 2). In order to obtain ligands with similar shape, similar steric hindrance and close molecular weights, which is essential for their comparison *in vitro*, we opted to substitute *c*[-RGDfK-] for non sense *c*[-RβADfK-] motifs in the ligands whose valency was lower than four (compounds 2–5). We also designed a broad hexadecavalent ligand (compound 6) in order to compare the tetrameric RAFT(*c*[-RGDfK-])<sub>4</sub> with a dendrimer-like structure.

The first part of our work was dedicated to devising a modular synthetic strategy that would provide an easy access to molecules bearing one up to sixteen RGD ligands. The second part focused on the evaluation of the binding ability of these molecules to  $\alpha_v\beta_3$  receptors *in vitro*. RAFT(*c*[-RGDfK-])<sub>n</sub> derivatives have been comparatively assayed on  $\alpha_v\beta_3$ -expressing cells in order to pinpoint the influence of the cluster valency in the recognition process.

<sup>a</sup>Ingénierie Moléculaire et Chimie Bioorganique, LEDSS, CNRS UMR 5616, ICMG FR 2607, Université Joseph Fourier, BP 53, 38041 Grenoble Cedex 9, France. E-mail: Pascal.Dumy@ujf-grenoble.fr; Fax: (+33) 476-514-946; Tel: (+33) 476-635-545

<sup>b</sup>Groupe de Recherche sur le Cancer du Poumon, INSERM U578, Institut Albert Bonniot IFR 73, Domaine de la Merci, 38706 La Tronche Cedex, France

† Electronic supplementary information (ESI) available: RP-HPLC chromatograms and ESI-MS spectra of purified peptides and conjugated compounds. See DOI: 10.1039/b517706e

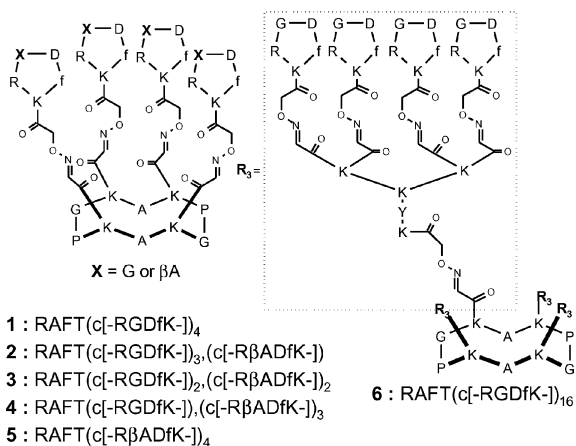


Fig. 2 Chemical structures of the RAFT(c[-RGDfK-])<sub>n</sub> ligands.

## Results and discussion

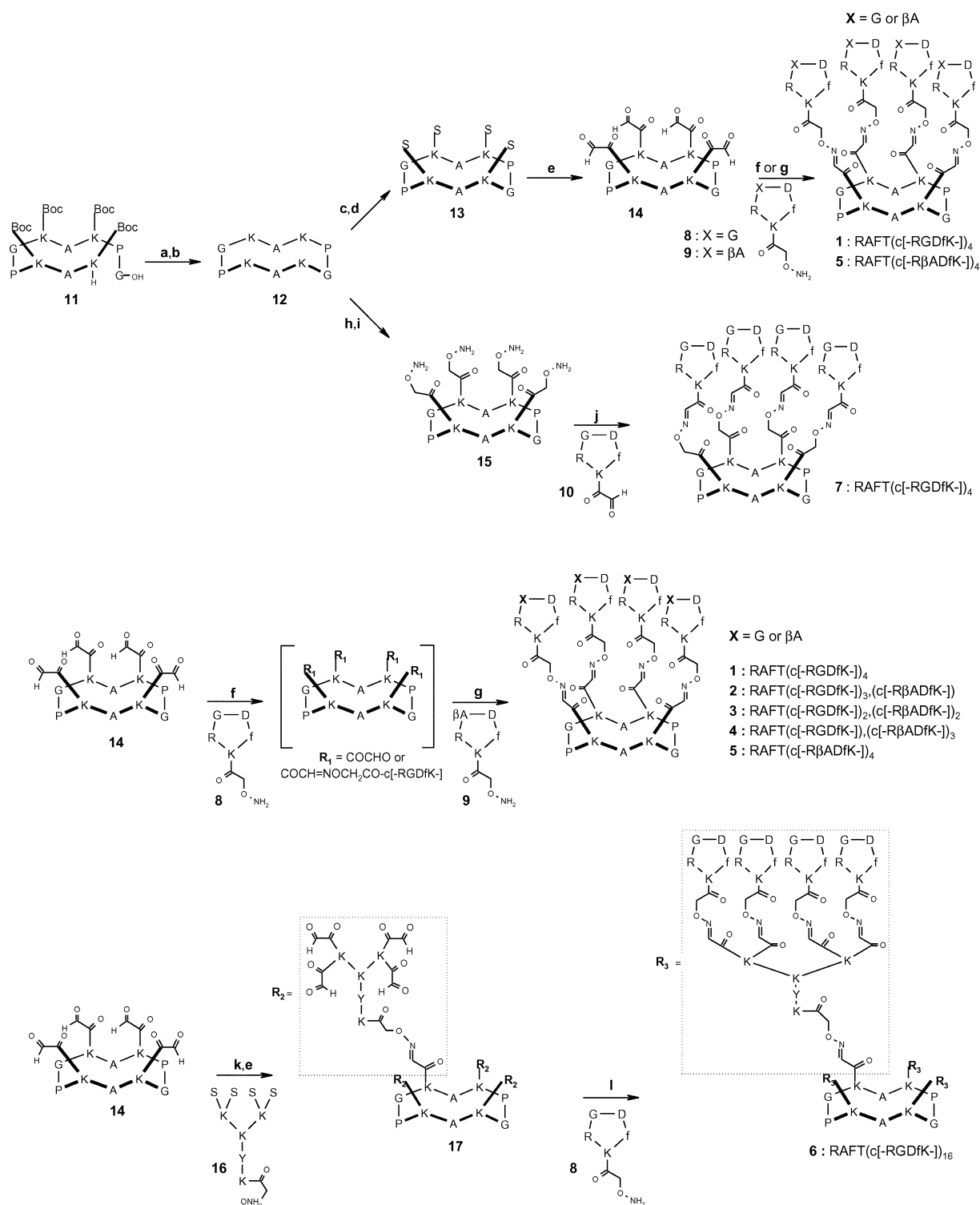
### Synthesis of the multivalent RGD peptides: RAFT(c[-RGDfK-])<sub>n</sub>, n = {1,2,3,4,16}

To design our molecules, displaying one up to sixteen c[-RGDfK-] motifs, we adopted the modular strategy described earlier.<sup>8</sup> We selected cyclic decapeptide RAFTs,<sup>10</sup> containing addressable lysine side chains, to present the multiple RGD monomers in a spatially controlled domain. We implemented chemoselective oxime formations to link the c[-RGDfK-] peptides onto the RAFT scaffold. Previous work has demonstrated the efficiency and versatility of the oxime linkage when performing the synthesis of bioconjugates especially when conjugating peptides, carbohydrates and oligonucleotides.<sup>13</sup> This approach allows unprotected fragments bearing adequate functions (*i.e.* aldehyde and aminoxy groups) to be assembled in aqueous solution without the requirement of any coupling reagent nor the occurrence of any side reaction.

Following this general strategy, we synthesized an array of RGD-containing peptides 1–7 (Scheme 1): (i) Peptides 1–4 were produced to study the effect of the cluster valency index toward the recognition and binding of the ligand to  $\alpha_v\beta_3$  integrins. Non sense c[-RβADfK-] motifs were substituted for c[-RGDfK-] in the structures whose valency was lower than four (compounds 2, 3 and 4). This enabled different multimers with similar shape, similar steric hindrance and comparable molecular weights to be obtained. These features are essential for further biological comparison of the ligands; (ii) The peptide 5 was mandatory as control for biological studies; (iii) The hexadecaivalent peptide 6 was designed to compare our ligands to a tentacular structure of high valency index; (iv) Peptide 7 was synthesized in order to ascertain that the polarity of the oxime bonds has no influence on the binding of the RGD motifs to the target receptors. Compounds 1–7 were synthesized following the synthetic routes described in Scheme 1. All linear peptides were assembled using the standard Fmoc/*t*Bu strategy on acid labile resins. The common intermediate 11 displays Boc-protected lysine side chains required to introduce the prerequisite groups (aldehyde or aminoxy functions further used in the chemoselective ligations with the cyclopentapeptides). Glycine at the C-terminal end was essential to ensure the subsequent head-to-tail cyclization from epimerisation. This reaction

was performed with PyBOP reagent under high dilution to avoid polymerisation as reported.<sup>8,14</sup> Removal of Boc groups using TFA provided the key intermediate 12 in quantitative yield. This compound constitutes the convergence point of the two synthetic ways considered to access the tetraivalent RAFT(c[-RGDfK-])<sub>4</sub> ligand. Incorporation of either aldehyde moieties or aminoxy groups leads to RAFT(c[-RGDfK-])<sub>4</sub> 1 or 7 respectively only differing in the cyclic decapeptide 12 was acylated on the lysine side chains with Boc-Ser(*t*Bu)OH amino acids serving as masked glyoxylyl aldehyde functions. Removal of acid-labile protecting groups and the subsequent oxidative cleavage of the amino-alcohol moiety at the serine residues with sodium periodate afforded the desired compound RAFT(COCHO)<sub>4</sub> 14 in good yield. On the other hand, the cyclopeptide 12 was acylated at the lysine side chains using the succinimide ester of *N*-Boc-*O*-(carboxymethyl)-hydroxylamine. Removal of Boc groups was further achieved by treatment with TFA containing triisopropylsilane (TIS) and water in CH<sub>2</sub>Cl<sub>2</sub> (50/5/5/40). RP-HPLC purification provided the tetra-aminoxy functionalised intermediate RAFT(COCH<sub>2</sub>ONH<sub>2</sub>)<sub>4</sub> 15 in 70% overall yield. In parallel, cyclic RGD-containing pentapeptides 8 and 10 and the non sense cyclic RβAD-containing pentapeptide 9 were produced by a two-dimensional solid phase synthesis as described earlier.<sup>14</sup> Final chemoselective assembly of fully deprotected fragments was carried out using both partners (*i.e.* RAFT scaffold and cyclic pentapeptide) containing either aminoxy or aldehyde functions. Chemoselective oxime ligations were carried out under mild conditions at pH 4.5 (sodium acetate buffer).

Compound 14 exhibiting four glyoxylyl aldehydes was preferred to its aminoxy counterpart 15 to synthesize the different RGD-containing peptides 1–6. In fact, reactions with clustered aldehydes are often cleaner than those effected with clustered aminoxy groups due to the risks of contamination by solvents commonly used in the laboratory (*e.g.* acetone, alcohol), even when special care is taken. RAFT(c[-RGDfK-])<sub>4</sub> 1 and control RAFT(c[-RβADfK-])<sub>4</sub> 5 were efficiently obtained through ligation of the appropriate cyclic pentapeptide containing aminoxy functions, namely c[-RGDfK(COCH<sub>2</sub>ONH<sub>2</sub>)] 8 and c[-RβADfK(COCH<sub>2</sub>ONH<sub>2</sub>)] 9, with 14 in 76% and 80% yield respectively. The RAFT(c[-RGDfK-])<sub>4</sub> 7, that differs from 1 only in the orientation of the oxime bonds, was obtained from the aminoxy intermediate RAFT(COCH<sub>2</sub>ONH<sub>2</sub>)<sub>4</sub> 15 and the RGD-containing cyclic pentapeptide 10 in a similar way to 1. To provide all peptides 2–4 exhibiting 1, 2 or 3  $\alpha_v\beta_3$  ligands, we opted to build mixtures of compounds consisting of isomers that differ in the position of the cyclic RGD pentapeptides onto the RAFT. This combinatorial assembling strategy was essential to explore all possible positions of the RGD motifs. The mixtures thus contain two isomers for peptides 2 and 4 and four isomers for peptide 3. It is important to note that the different isomers within the mixture may display differences in the binding assay. We easily accessed each mixture in two steps from 14. We firstly used 0.25 equivalent (per aldehyde site of 14) of c[-RGDfK(COCH<sub>2</sub>ONH<sub>2</sub>)] 8 to graft RGD moieties onto the scaffold. The reaction was monitored by RP-HPLC (Fig. 3). Each intermediate of the reaction was identified by mass spectrometry and revealed to be the mono, the bis and the tris c[-RGDfK-] conjugated compounds (including different isomers). These were easily isolated after separation by RP-HPLC. The conditions used did not allow the separation of



**Scheme 1** Reagents and conditions: (a) PyBOP, DIPEA, DMF; (b) TFA/CH<sub>2</sub>Cl<sub>2</sub> (1 : 1); (c) BocSer(*t*Bu)OH, PyBOP, DIPEA, DMF; (d) TFA/CH<sub>2</sub>Cl<sub>2</sub> (9 : 1); (e) NaIO<sub>4</sub>, H<sub>2</sub>O; (f) for **1** : **8**, CH<sub>3</sub>CN/AcO<sup>-</sup>Na<sup>+</sup> (0.1 M, pH 4.5) (1 : 2) and for **2–4** : **8**, AcO<sup>-</sup>Na<sup>+</sup> (0.1 M, pH 4.5); (g) for **5** : **9**, AcO<sup>-</sup>Na<sup>+</sup> (0.1 M, pH 4.5); (h) BocNHCH<sub>2</sub>CO-Succ, DIPEA, DMF; (i) TFA/CH<sub>2</sub>Cl<sub>2</sub>/TIS/H<sub>2</sub>O (10 : 8 : 1 : 1); (j) **10**, CH<sub>3</sub>CN/H<sub>2</sub>O (1 : 1); (k) **16**, CH<sub>3</sub>CN/AcO<sup>-</sup>Na<sup>+</sup> (0.1 M, pH 4.0) (1 : 1); (l) **8**, CH<sub>3</sub>CN/AcO<sup>-</sup>Na<sup>+</sup> (0.1 M, pH 4.0) (5 : 1).

the different isomers. The subsequent reactions with non sense c[-R $\beta$ ADfK(COCH<sub>2</sub>ONH<sub>2</sub>)-] **9** furnished the desired peptides **2–4** in reasonable yields. All peptides were characterized by mass spectrometry without ambiguity.

To extend the multivalency to sixteen  $\alpha$ <sub>3</sub> $\beta$ <sub>3</sub> ligands, we prepared the polylysine peptide **16** containing an oxyamino group, allowing the anchoring to the scaffold **14**, and four masked aldehyde functions (serine residues) at the  $\alpha$  and  $\epsilon$  amines of the N-terminal

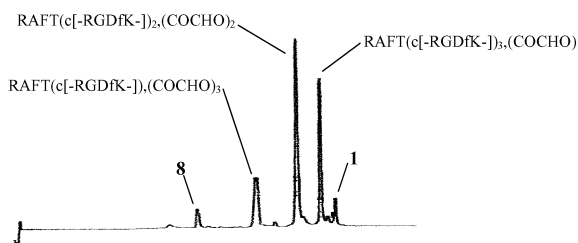


**Fig. 3** RP-HPLC profile of the reaction between **14** and 0.25 equivalent (per aldehyde group) of **8** after 2 h.

lysines. This kind of peptide has been extensively exploited for the preparation of synthetic vaccines.<sup>15</sup> The first chemoselective ligation step between the scaffold **14** and four peptides **16** and the subsequent oxidation of the sixteen serine residues provided RAFT(COCHO)<sub>16</sub> **17** in an excellent 93% overall yield. The second chemoselective ligation step using *c*[-RGDfK[COCH<sub>2</sub>ONH<sub>2</sub>]-] **8** afforded the RAFT(*c*[-RGDfK-])<sub>16</sub> **6** in excellent yield. The macromolecule was characterised by mass spectrometry (Fig. 4). The deconvoluted mass was found in perfect agreement with the calculated mass (15614.9).

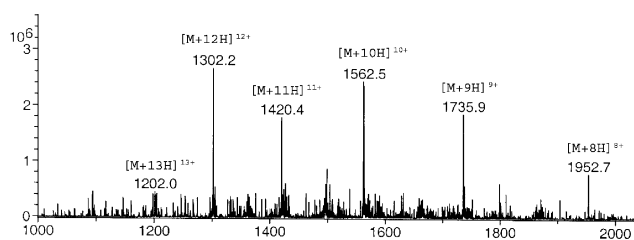


**Fig. 4** Mass spectrum of **6**.

### Biological assays

The adhesion potency of the different multivalent RGD-containing peptides was initially determined using a traditional solid phase ELISA-type inhibition assay. In this assay, we comparatively measured their efficiency to compete with vitronectin (the natural substrate of  $\alpha_v\beta_3$  integrin) when binding to the  $\alpha_v\beta_3$  cellular receptor. CHO-3a cells were thus incubated with soluble RAFT(*c*[-RGDfK-])<sub>n</sub> ligands at 37 °C onto vitronectin-coated assay plates.

The comparative analysis of the different peptides is reported in Table 1 (Competitive cell adhesion assay). As expected the negative control peptide **5** did not inhibit cell adhesion to vitronectin. IC<sub>50</sub> values show that increasing the number of *c*[-RGDfK-] motifs onto the RAFT from 1 to 4 gradually improved the potency of the ligand to compete with vitronectin. A slight difference was observed between compounds **1** and **2** (IC<sub>50</sub> of 0.58  $\mu$ M and 0.66  $\mu$ M respectively). The monovalent RGD-containing peptide **4** showed the highest IC<sub>50</sub> value. Nevertheless, related to the number of RGD ligand exposed on each structure, we found that the relative binding potency of each RGD unit for clustered peptide **1** is lower than those of univalent ligands **4** and *c*[-RGDfK-]. Recently, internalization of clustered tetravalent RGD-containing peptide was visualized at 37 °C in CHO-3a and HUVEC cells, whereas low uptake was observed in the case of the monovalent RGD peptide.<sup>8,11</sup> For this reason, this test is potentially misleading in comparing the binding affinity of the monovalent molecules with the clustered molecules. In this context, it was essential to consider a cellular assay that was feasible at 4 °C to prevent the uptake of peptides.<sup>16</sup>

We then measured the capacity of the peptides to inhibit the recognition of the  $\alpha_v\beta_3$ -specific 23C6 monoclonal antibody (23C6 mAb) on HEK293( $\beta_3$ ) cells. HEK293( $\beta_3$ ) were chosen for their high expression levels of  $\alpha_v\beta_3$  integrins. Fig. 5a (control) shows the level of  $\alpha_v\beta_3$  integrins after immunostaining of cells with 23C6 mAb conjugated to R-Phycoerythrin and FACS quantification. In the condition where the cells were previously incubated for 30 min at 4 °C with 250 nM of the clustered peptide **1**, the fluorescence signal was significantly shut down (Fig. 5c). This result indicated that the interaction of peptide **1** with  $\alpha_v\beta_3$  integrin abolished the recognition of 23C6 mAb. This phenomenon was

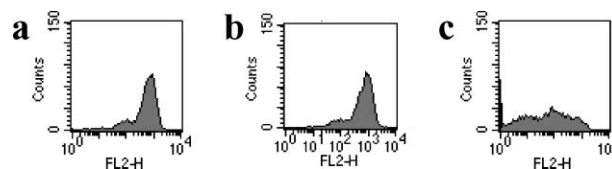


**Fig. 5** 23C6 mAb-R-Phycoerythrin fluorescence (FL2) histogram counts of cell suspensions incubated for 30 min. at 4 °C with (a) PBS Mg<sup>2+</sup> (1 mM), (b) *c*[-RGDfK-] 20  $\mu$ M or (c) RAFT(*c*[-RGDfK-])<sub>4</sub> 0.25  $\mu$ M.

**Table 1** Determination of the IC<sub>50</sub> values and the relative inhibitory capacity (Relative Potency, Rel. Pot.) of (i) peptides **1–5** to CHO-3a cell adhesion in a solid phase assay with surface immobilized vitronectin at 37 °C and (ii) peptides **1–6** to HEK293( $\beta_3$ ) cell staining in solution with 23C6 monoclonal antibody (mAb) at 4 °C

| Peptides           | RGD units per molecule | Competitive cell adhesion assay <sup>(i)</sup> : |                        | Inhibition of $\alpha_v\beta_3$ -specific 23C6 mAb staining assay <sup>(ii)</sup> : |                        |
|--------------------|------------------------|--|------------------------|---|------------------------|
|                    |                        | IC <sub>50</sub> ( $\mu$ M) <sup>a</sup>         | Rel. Pot. <sup>b</sup> | IC <sub>50</sub> /nM  | Rel. Pot. <sup>b</sup> |
| <i>c</i> [-RGDfK-] | 1                      | 0.93 $\pm$ 0.03                                  | 62 (62)                | inactive  | inactive               |
| <b>1</b>           | 4                      | 0.58 $\pm$ 0.03                                  | 100 (25)               | 19  | 100 (25)               |
| <b>2</b>           | 3                      | 0.66 $\pm$ 0.01                                  | 88 (29)                | 36  | 53 (18)                |
| <b>3</b>           | 2                      | 0.99 $\pm$ 0.03                                  | 59 (30)                | 250   | 8 (4)                  |
| <b>4</b>           | 1                      | 1.28 $\pm$ 0.08                                  | 45 (45)                | >20000  | >0.1                   |
| <b>5</b>           | 0                      | inactive   | inactive               | —   | —                      |
| <b>6</b>           | 16                     | —  | —                      | 112   | 17 (1)                 |

<sup>a</sup> IC<sub>50</sub> values calculated from duplicates. <sup>b</sup> The numbers in parentheses express the relative potency per RGD unit in the ligands that contain more than one RGD motif.

not observed either with the control peptide **5** (data not shown) or with the monovalent  $c[-\text{RGDfK-}]$  ligand even at high doses (20  $\mu\text{M}$ ) (Fig. 5b). We thus reasoned that the tetravalent structure hides the epitope of the antibody but not  $c[-\text{RGDfK-}]$ . It is worth noting that this assay does not corroborate the biological activity of  $c[-\text{RGDfK-}]$  probably due to a smaller contact surface with the integrin compared to the antibody as inferred by the X-ray structure of the binding complex.<sup>17</sup> Therefore this assay was especially used to discriminate the different binding surfaces provided by  $\text{RAFT}(c[-\text{RGDfK-}])_n$  compounds in order to give an account of their ability to interact with  $\alpha_v\beta_3$  integrins. Cell suspensions were incubated with different concentrations of peptides **1–7** at 4 °C, stained with the fluorescent  $\alpha_v\beta_3$ -specific 23C6 mAb and analysed by FACS.

We first established that  $\text{RAFT}(c[-\text{RGDfK-}])_4$  peptides **1** and **7**, that differ in the oxime orientation, have a similar interaction with  $\alpha_v\beta_3$  receptors as these show the same inhibition profiles (Fig. 6). This result is of significant importance for insuring the complete modularity of our synthetic strategy. The assay also revealed a nice dose-dependant inhibition of integrin recognition with an extinction concentration around 0.1  $\mu\text{M}$ . Table 1 summarizes all compounds as evaluated in the inhibition of 23C6 mAb staining assay. A slight difference was again observed between compounds **1** and **2** ( $\text{IC}_{50}$  of 19 nM and 36 nM respectively). Decreasing the number of RGD units on the scaffold reduced dramatically the inhibition of 23C6 mAb recognition of more than 1000-fold for **4**. The increase of the relative potency of RAFT peptide from **4** to **1** reveals a significant multivalency effect with at least 250-fold enhancement. The multivalent peptide **6** surprisingly showed no significant multivalency effect as its relative potential of inhibition is close to the one observed for **3**. The proximity of the RGD units of peptide **6** and the steric hindrance in between may be the reason for the lack of affinity of the large multivalent structure. Increasing the length of the linker between RGD motif and the lysine of the RAFT scaffold is under investigation.

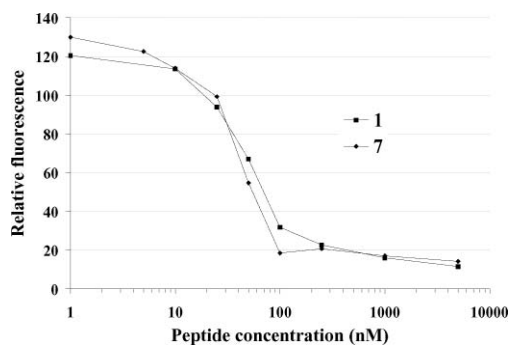


Fig. 6 Inhibition of 23C6 MAb immunostaining by **1** and **7**.

As the steric hindrance is roughly the same for peptides **1–7** (except **6**), this assay clearly demonstrated that clustered RGD ligand grafted onto the RAFT scaffold strengthened the binding of the molecule to the integrin excepted for compound **6** presenting sixteen RGD units. We hypothesize that the multivalent effect observed with the integrin results from a mechanism that involves a statistical rebinding of the RGD units, a phenomenon observed for glycodendrimers.<sup>18</sup> At an identical concentration in RGD units, this mechanism is highly in favour of clustered

molecules (compounds **1** and **2**) rather than of univalent molecules (compound **4**). To our knowledge, at the low temperature used for this assay, the multivalent effect observed could not be attributed to  $\alpha_v\beta_3$  receptors clustering.

## Conclusions

A modular strategy to prepare an array of peptides displaying RGD units is here described. Several parameters were studied and especially the effect of a clustered ligand presentation onto a RAFT scaffold using cells expressing  $\alpha_v\beta_3$  integrins. In the literature, most studies of  $\alpha_v\beta_3$  integrin adhesion were accomplished on the purified integrin *in vitro* and few data *in vivo* are available. To evaluate our molecules, it was essential to set up experiments at low temperature to limit the uptake of peptides. Use of the  $\alpha_v\beta_3$ -specific 23C6 monoclonal antibody indirectly permitted the comparison of the affinities of the ligands towards the integrin. The results obtained highlight the utility of a clustered ligand. Nevertheless, it is worth noting that the length of the linker between the ligand and the scaffold might be very important for limiting the steric hindrance due to the proximity between ligand moieties. From these observations,  $\text{RAFT}(c[-\text{RGDfK-}])_{3,4}$  are considered as potent  $\alpha_v\beta_3$  integrin ligands that can find applications in tumour-targeted drugs or probe delivery.

## Experimental

### Materials

Protected amino acids and Sasrin<sup>TM</sup> resin were obtained from Advanced ChemTech Europe (Brussels, Belgium), Bachem Biochimie SARL (Voisins-Les-Brettonneux, France), Merck Eurolab (Fontenay-sous-Bois, France) and France Biochem S.A. (Meudon, France). PyBOP was purchased from France Biochem and other reagents either from Aldrich (Saint-Quentin Fallavier, France) or from Acros (Noisy-Le-Grand, France). RP-HPLC were performed on Waters equipment consisting of a Waters 600 controller and a Waters 2487 Dual Absorbance Detector. Analyses were performed on an analytical column (Macherey-Nagel Nucleosil 100 Å 5  $\mu\text{m}$  C<sub>18</sub> particles, 250 × 4.6 mm) using the following system of solvent: solvent A, 0.09% TFA in water; solvent B, 0.09% TFA/9.91% H<sub>2</sub>O in 90% acetonitrile; flow rate, 1.0 mL min<sup>-1</sup> with UV monitoring at 214 nm and 250 nm. Preparative column (Delta-Pak<sup>TM</sup> 300 Å 15  $\mu\text{m}$  C<sub>18</sub> particles, 200 × 2.5 mm) was used with an identical system of solvents at a flow rate of 22 mL min<sup>-1</sup>. Mass spectra were obtained by electron spray ionization (ES-MS) on a VG Platform II (Micromass).

### General procedure for solid-phase peptide synthesis

Assembly of protected peptides was carried out using the Fmoc/*t*-Bu strategy manually in a glass reaction vessel fitted with a sintered glass frit, or automatically on a synthesizer (348  $\Omega$  synthesizer, Advance ChemTech). Coupling reactions were performed using, relative to the resin loading, 1.5–2 eq. of *N*- $\alpha$ -Fmoc protected amino acid activated *in situ* with 1.5–2 eq. PyBOP and 3–4 eq. diisopropylethylamine (DIPEA) in DMF (10 mL g<sup>-1</sup> resin) for 30 min. Manual syntheses were controlled by Kaiser and/or TNBS tests. *N*- $\alpha$ -Fmoc protecting groups were removed by treatment

with a piperidine/DMF solution (1:4) (10 mL g<sup>-1</sup> resin) for 10 min. The process was repeated three times and the completeness of deprotection verified by the UV absorption of the piperidine washings at 299 nm. Synthetic linear peptides were recovered directly upon acid cleavage (1% TFA in CH<sub>2</sub>Cl<sub>2</sub>). Resins were treated for 3 min repeatedly until the resin beads became dark purple. The combined washings were concentrated under reduced pressure and white solid peptides were obtained by precipitation from ether. They were analyzed by RP-HPLC, and if necessary purified on a preparative column.

**Peptide derivatives 8, 9, 10 and 16.** Compounds **8**, **9**, **10** and **16** were prepared as described in the literature by a combination of SPPS and solution strategy.<sup>10</sup>

**RAFT derivative 12.** The linear decapeptide H-Lys(Boc-Ala-Lys(Boc)-Pro-Gly-Lys(Boc)-Ala-Lys(Boc)-Pro-Gly-OH **11** was prepared from Sasrin<sup>TM</sup> resin (500 mg, 0.53 mmol g<sup>-1</sup>). Cyclization of the linear peptide (0.5 mM) was performed in DMF by adding PyBOP (1.2 eq.) as described.<sup>8</sup> Boc groups were removed in a solution containing TFA/CH<sub>2</sub>Cl<sub>2</sub> (1 : 1) providing compound **12** as a white powder in quantitative yield. Mass spectrum (ES-MS, positive mode) calcd 963.2, found 963.3.

**RAFT derivative 13.** To a solution containing compound **12** (150 mg, 0.1 mmol) in 10 mL of DMF were added Boc-Ser(tBu)OH (130.5 mg, 0.5 mmol) and DIPEA to adjust the pH at 8.0. The reaction was stirred for 30 min. at room temperature and concentrated under reduced pressure. The crude material was washed with ether and a solution of 10 mL of TFA/CH<sub>2</sub>Cl<sub>2</sub> (9 : 1) was added. After 1 hour, the reaction was concentrated under reduced pressure and peptide **13** precipitated from ether (160 mg, 90.5 μmol, 91% overall yield). Mass spectrum (ES-MS, positive mode) calcd 1311.5, found 1311.6.

**RAFT derivative 14.** To a solution containing compound **13** (160 mg, 90.5 μmol) in 10 mL of water was added NaIO<sub>4</sub> (64 mg, 0.3 mmol). The reaction was stirred for 30 min. at room temperature. The product was then purified by RP-HPLC to afford compound **14** as a white powder (80 mg, 67 μmol, 75%). Mass spectrum (ES-MS, positive mode) calcd 1187.3, found 1186.7.

**RAFT derivative 15.** To a solution containing compound **12** (151 mg, 0.11 mmol) in 10 mL of DMF were added Boc-NHOCH<sub>2</sub>CO-Succ (134 mg, 0.47 mmol) and DIPEA to adjust the pH at 8.0. The reaction was stirred for 30 min. at room temperature and then concentrated under reduced pressure. The crude product was washed with ether and a solution of 10 mL of TFA/CH<sub>2</sub>Cl<sub>2</sub>/TIS/H<sub>2</sub>O (10 : 8 : 1 : 1) was added. After 1 hour, the reaction was concentrated under reduced pressure and peptide **15** purified from RP-HPLC (127 mg, 70 μmol, 70% overall yield). Mass spectrum (ES-MS, positive mode) calcd 1255.4, found 1255.5.

**RAFT(c[-RGDfK-])41.** To a solution containing the derivative **14** (10.6 mg, 8.9 μmol) in 2.7 mL of sodium acetate buffer (0.1 M, pH 4.5)/acetonitrile (2:1) was added the peptide **8** (39.0 mg, 43.0 μmol). The reaction was stirred for 3 h. at 25 °C. Conjugate

**1** was isolated after purification using RP-HPLC as a white powder (25.7 mg, 6.7 μmol, 76%). Purity (assessed by HPLC) 100%. Mass spectrum (ES-MS, positive mode) calcd 3822.2, found 3821.7.

**RAFT(c[-RGDfK-])32.** To a solution containing the derivative **14** named RAFT(COCHO)<sub>4</sub> (10.0 mg, 8.4 μmol) in 8 mL of sodium acetate buffer (0.1 M, pH 4.5) was added the peptide **8** (8.8 mg, 9.6 μmol). The reaction was stirred for 6 h. at 25 °C. Conjugates with 1, 2 and 3 c[-RGDfK-] residues were isolated using RP-HPLC affording RAFT(c[-RGDfK-]),(COCHO)<sub>3</sub> (4.6 mg, 2.3 μmol, 28%), RAFT(c[-RGDfK-])<sub>2</sub>,(COCHO)<sub>2</sub> (5.0 mg, 1.8 μmol, 21%) and RAFT(c[-RGDfK-])<sub>3</sub>,(COCHO) (3.0 mg, 0.9 μmol, 11%). Mass spectra respectively (ES-MS, positive mode) calcd 1900.1, found 1899.6; calcd 2540.9, found 2541.0; calcd 3181.5, found 3180.2.

To a solution containing the RAFT(c[-RGDfK-])<sub>3</sub>,(COCHO) (3.0 mg, 0.9 μmol) in 0.5 mL of sodium acetate buffer (0.1 M, pH 4.5) was added the peptide **9** (1.2 mg, 1.4 μmol). The reaction was stirred for 5 h. at 25 °C. Conjugate **2** was isolated after purification using RP-HPLC as a white powder (2.7 mg, 0.6 μmol, 67%). Purity (assessed by HPLC) 100%. Mass spectrum (ES-MS, positive mode) calcd 3836.2, found 3837.2.

**RAFT(c[-RGDfK-])2 3.** To a solution containing the RAFT(c[-RGDfK-])<sub>2</sub>,(COCHO)<sub>2</sub> (5.0 mg, 1.8 μmol) in 1 mL of sodium acetate buffer (0.1 M, pH 4.5) was added the peptide **9** (4.9 mg, 5.4 μmol). The reaction was stirred for 5 h. at 25 °C. Conjugate **3** was isolated after purification using RP-HPLC as a white powder (5.2 mg, 1.2 μmol, 67%). Purity (assessed by HPLC) 97%. Mass spectrum (ES-MS, positive mode) calcd 3850.2, found 3849.9.

**RAFT(c[-RGDfK-])1 4.** To a solution containing the RAFT(c[-RGDfK-]),(COCHO)<sub>3</sub> (4.6 mg, 2.3 μmol) in 1 mL of sodium acetate buffer (0.1 M, pH 4.5) was added the peptide **9** (9.6 mg, 10.4 μmol). The reaction was stirred for 5 h. at 25 °C. Conjugate **4** was isolated after purification using RP-HPLC as a white powder (6.1 mg, 1.4 μmol, 61%). Purity (assessed by HPLC) 97%. Mass spectrum (ES-MS, positive mode) calcd 3864.3, found 3865.2.

**RAFT(c[-RβADfK-])4 5.** To a solution containing the derivative **14** (9.3 mg, 7.8 μmol) in 2.5 mL of sodium acetate buffer (0.1 M, pH 4.5) was added the peptide **9** (38.0 mg, 46.8 μmol). The reaction was stirred for 3 h. at 25 °C. Conjugate **5** was isolated after purification using RP-HPLC as a white powder (24.1 mg, 6.2 μmol, 80%). Purity (assessed by HPLC) 100%. Mass spectrum (ES-MS, positive mode) calcd 3878.3, found 3878.3.

**RAFT(c[-RGDfK-])16 6.** To a solution containing the compound **14** (5 mg, 4.3 μmol) in 1 mL of sodium acetate buffer (0.1 M, pH 4.0)/acetonitrile (1 : 1) was added the peptide **16** (33 mg, 19.5 μmol). The reaction was stirred for 2 h. at room temperature. The product was isolated after a purification by RP-HPLC as a white powder. To a solution containing this compound (31.9 mg, 4.0 μmol) in 8 mL of aqueous solution was added sodium periodate (18.5 mg, 86 μmol). The reaction was stirred for 1 h. at room temperature. The intermediate compound **17** was purified

by RP-HPLC and isolated as a white powder in quantitative yield (20.6 mg, 4.0  $\mu\text{mol}$ , 93% overall yield). Compound **17** (14.5 mg, 2.86  $\mu\text{mol}$ ) was then dissolved in 6 mL of a solution containing sodium acetate buffer (0.1 M, pH 4.0)/acetonitrile (5 : 1). RGD derivative **8** (62.1 mg, 68.6  $\mu\text{mol}$ ) was added and the reaction was stirred for 24 h. Hexadecavalent derivative **6** was isolated after purification by RP-HPLC as a white powder (42.8 mg, 2.45  $\mu\text{mol}$ , 86%). Purity (assessed by HPLC) 100%. Mass spectrum (ES-MS, positive mode) calcd 15614.9, found 15614.9.

**RAFT(c[RGDfK]-)47.** To a solution containing the derivative **15** (16.2 mg, 9.5  $\mu\text{mol}$ ) in 2.2 mL of water/acetonitrile (1 : 1) was added the peptide **10** (34.6 mg, 44.7  $\mu\text{mol}$ ). The reaction was stirred for 4 h. at 25 °C. Conjugate **7** was isolated after purification using RP-HPLC as a white powder (18.7 mg, 4.4  $\mu\text{mol}$ , 47%). Purity (assessed by HPLC) 93%. Mass spectrum (ES-MS, positive mode) calcd 3822.2, found 3822.6.

### Cell lines and culture conditions

CHO-3a cells, stable transfectants of human  $\beta_3$  subunit from the Chinese hamster ovary cell line, were kindly supplied by A. Duperray (INSERM U578, IAB, Grenoble). The CHO-3a clone was cultured in Dulbecco's Modified Eagles Medium (DMEM) supplemented with 10% heat-inactivated fetal calf serum (FCS), penicillin (50 U mL<sup>-1</sup>), streptomycin (50  $\mu\text{g mL}^{-1}$ ) and 400  $\mu\text{g mL}^{-1}$  G418. HEK293( $\beta_3$ ) cells, stable transfectants of human  $\beta_3$  subunit from the human embryonic kidney cell line, were kindly supplied by J-F. Gourvest (Aventis, France). They were cultured in DMEM enriched with 4.5 g L<sup>-1</sup> glucose and supplemented with 1% glutamine, 10% FCS, penicillin (50 U mL<sup>-1</sup>), streptomycin (50  $\mu\text{g mL}^{-1}$ ) and 700  $\mu\text{g mL}^{-1}$  G418. Cells were maintained at 37 °C in a humidified atmosphere of 5% CO<sub>2</sub>.

### Competitive cell adhesion assays

96-well assay plates (Maxisorb NUNC™) were coated for 1 h. at room temperature with 5  $\mu\text{g mL}^{-1}$  vitronectin in PBS and blocked for 30 min. at room temperature with 3% bovine serum albumin (BSA) in PBS. Varying amounts of peptides were added simultaneously with 10<sup>5</sup> trypsinated CHO-3a cells to the wells and the plate was incubated for 45 min. at 37 °C. Wells were rinsed three times with PBS in order to remove vitronectin-unbound cells. Attached cells were then fixed with methanol, stained with methylene blue and quantified by OD reading at 630 nm on a Dynatech MR5000 plate reader. The activity of peptides is expressed as IC<sub>50</sub> values (concentration of peptide necessary to inhibit 50% of cell attachment to the vitronectin substrate) which were determined from inhibition profiles.

### Inhibition of $\alpha\text{V}\beta_3$ -specific antibody fixation assay

Trypsinated HEK293( $\beta_3$ ) cells were incubated with varying concentrations of peptides in PBS enriched with 1 mM MgCl<sub>2</sub> at 4 °C for 30 min. (10<sup>6</sup> cells-200  $\mu\text{L}$ ). Cells were rinsed twice with cold PBS before being incubated with R-Phycoerythrin-conjugated 23C6 monoclonal antibody in 1% BSA/PBS/MgCl<sub>2</sub> (1 mM) for another 30 min. at 4 °C. After being rinsed twice with cold PBS, cells were

fixed with 0.5% paraformaldehyde in PBS for 10 min. at 4 °C. Cells were finally rinsed once with cold PBS and resuspended in 1 mL PBS for flow cytometry analysis. FACS measurements were carried out using a FACScan (Becton Dickinson) and the results presented are expressed as mean fluorescent intensity (relative fluorescence) of 10,000 collected cells.

### Acknowledgements

We thank the Association pour la Recherche contre le Cancer (ARC N° 3741), the Ministère de la Recherche (ACI N° 02L0525), the Région Rhône-Alpes (N° 0301372501 and 0301372502), the Cancéropôle (N° 032115 and 042259), the Université Joseph Fourier, the Centre National de la Recherche Scientifique (CNRS), the Institut National de la Santé Et de la Recherche Médicale (INSERM) and the Institut Universitaire de France (IUF) for supporting this work. Financial assistance from La Ligue Nationale Contre le Cancer (to E. G.) is gratefully acknowledged.

### References

- (a) F. G. Giancotti and E. Ruoslahti, *Science*, 1999, **285**, 1028–1032; (b) M. J. Humphries, *Biochem. Soc. Trans.*, 2000, **28**, 311–339; (c) R. O. Hynes, *Nat. Med.*, 2002, **8**, 918–921.
- P. C. Brooks, A. M. Montgomery, M. Rosenfeld, R. A. Reisfeld, T. Hu, G. Klier and D. A. Cheresh, *Cell*, 1994, **79**, 1157–1164.
- (a) M. A. Dechantsreiter, E. Planker, B. Mathä, E. Lohof, G. Hölzemann, A. Jonczyk, S. L. Goodman and H. Kessler, *J. Med. Chem.*, 1999, **42**, 3033–3040; (b) J. W. Smith, *Curr. Opin. Invest. Drugs (Thomson Sci.)*, 2003, **4**, 741–745.
- M. Mammen, S. K. Choi and G. M. Whitesides, *Angew. Chem., Int. Ed.*, 1998, **37**, 2754–2794.
- G. Thumshirn, U. Hersel, S. L. Goodman and H. Kessler, *Chem.-Eur. J.*, 2003, **9**, 2717–2725.
- T. Poethko, M. Schottelius, G. Thumshirn, M. Herz, R. Haubner, G. Henriksen, H. Kessler, M. Schwaiger and H.-J. Wester, *Radiochim. Acta*, 2004, **92**, 317–327.
- H.-J. Wester and H. Kessler, *J. Nucl. Med.*, 2005, **12**, 1940–1945.
- D. Boturyn, J.-L. Coll, E. Garanger, M.-C. Favrot and P. Dumy, *J. Am. Chem. Soc.*, 2004, **126**, 5730–5739.
- (a) R. Haubner, R. Gratias, B. Diefenbach, S. L. Goodman, A. Jonczyk and H. Kessler, *J. Am. Chem. Soc.*, 1996, **118**, 7461–7472; (b) For a review, see: R. Haubner, D. Finsinger and H. Kessler, *Angew. Chem., Int. Ed. Engl.*, 1997, **36**, 1375–1389.
- (a) P. Dumy, I. Eggleston, S. Servigni, U. Sila, X. Sun and M. Mutter, *Tetrahedron Lett.*, 1995, **36**, 1255–1258; (b) M. Mutter, P. Dumy, P. Garroute, C. Lehmann, M. Mathieu, C. Peggion, S. Peluso, A. Razaname and G. Tuchscherer, *Angew. Chem., Int. Ed. Engl.*, 1996, **35**, 11482–11485; (c) S. Peluso, P. Dumy, C. Nkubana, Y. Yokokawa and M. Mutter, *J. Org. Chem.*, 1999, **64**, 7114–7120; (d) L. Scheibler, P. Dumy, D. Stamou, C. Duschl, H. Vogel and M. Mutter, *Tetrahedron*, 1998, **54**, 3725–3734; (e) L. Scheibler, P. Dumy, M. Boncheva, K. Leufgen, H. J. Mathieu, M. Mutter and H. Vogel, *Angew. Chem., Int. Ed.*, 1999, **38**, 696–699.
- E. Garanger, D. Boturyn, Z. Jin, P. Dumy, M.-C. Favrot and J.-L. Coll, *Mol. Ther.*, 2005, **12**, 1168–1175.
- (a) S. Castel, R. Pagan, F. Mitjans, J. Piulats, S. Goodman, A. Jonczyk, F. Huber, S. Vilaro and M. Reina, *Lab. Invest.*, 2001, **81**, 1615–1626; (b) A. J. Schraa, R. J. Kok, A. D. Berendsen, H. E. Moorlag, E. J. Bos, D. K. Meijer, L. F. de Leij and G. J. Molema, *J. Controlled Release*, 2002, **83**, 241–251.
- (a) D. Forget, D. Boturyn, E. Defrancq, J. Lhomme and P. Dumy, *Chem.-Eur. J.*, 2001, **7**, 3976–3984; (b) T. S. Zatsepin, D. A. Stetsenko, A. A. Arzumanov, E. A. Romanova, M. J. Gait and T. S. Oretskaya, *Bioconjugate Chem.*, 2002, **13**, 822–830; (c) O. Renaudet and P. Dumy, *Org. Lett.*, 2003, **5**, 243–246; (d) S. Grigalevicius, S. Chierici, O. Renaudet, R. Lo-Man, E. Deriaud, C. Leclerc and P. Dumy,

- 
- Bioconjugate Chem.*, 2005, **16**, 1149–1159; (e) Y. Singh, O. Renaudet, E. Defrancq and P. Dumy, *Org. Lett.*, 2005, **7**, 1359–1362.
- 14 D. Boturny and P. Dumy, *Tetrahedron Lett.*, 2001, **42**, 2787–2790.
- 15 (a) E. H. Nardin, J. M. Calvo-Calle, G. A. Oliveira, P. Clavijo, R. Nussenzweig, R. Simon, W. Zeng and K. Rose, *Vaccine*, 1998, **16**, 590–600; (b) J. Shao and J.-P. Tam, *J. Am. Chem. Soc.*, 1995, **117**, 3893–3899.
- 16 Competition test with vitronectin cannot be performed at 4 °C since cells are unable to adhere onto the vitronectin-coated plates at low temperature.
- 17 J.-P. Xiong, T. Stehle, R. Zhang, A. Joachimiak, M. Frech, S. L. Goodman and M. A. Arnaout, *Science*, 2002, **296**, 151–155.
- 18 J. E. Gestwicki, C. W. Cairo, L. E. Strong, K. A. Oetjen and L. L. Kiessling, *J. Am. Chem. Soc.*, 2002, **124**, 14922–14933.